University of Pennsylvania
ScholarlyCommons

Protocols and Reports

Browse by Type

1-30-2019

Dynamics of Directed Self-Assembly of PS-b-PMMA during Solvent Annealing

Hiromichi Yamamoto
Singh Center, hyam@seas.upenn.edu

Follow this and additional works at: https://repository.upenn.edu/scn_protocols

Part of the Engineering Commons, and the Physical Sciences and Mathematics Commons

Yamamoto, Hiromichi, "Dynamics of Directed Self-Assembly of PS-b-PMMA during Solvent Annealing", *Protocols and Reports.* Paper 54.
https://repository.upenn.edu/scn_protocols/54

This paper is posted at ScholarlyCommons. https://repository.upenn.edu/scn_protocols/54
For more information, please contact repository@pobox.upenn.edu.

Dynamics of Directed Self-Assembly of PS-b-PMMA during Solvent Annealing

Abstract

The graphoepitaxy of symmetric PS-b-PMMA BCP film on the PS 60 mol% brush layer is carried out using the chemically homogeneous topological pattern of SiO2 layer and the home-made solvent annealing tool. It is confirmed by atomic force microscopy that PS-b-PMMA film on the periphery of the trench flows into the trench during the solvent annealing, so that the film thickness in the trench is thicker than that on the un-patterned area. The solvent annealing time dependence indicates the lamellar orientation in the trench changes from a mixture of the lamellar domain parallel and perpendicular to the side walls to the lamellar domain parallel to the side walls, and then changes back to the mixture, although the lamellar orientation perpendicular to the substrate remains the same. This result is also discussed with a free energy model for confined di-block copolymer. The lamellar domain parallel to the side walls indicates that the surface tensions of PS and PMMA blocks absorbing solvent vapor with the PS 60 mol% brush layer are not the same during the solvent annealing at 55 °C. Furthermore, the free energy difference between the parallel and perpendicular orientations is supposed to fluctuate due to the dynamics of PS-b-PMMA molecules by the solvent annealing, so that the lamellar orientation results in either of the lamellar domain parallel, perpendicular, or the mixture.

Keywords

directed self-assembly, PS-b-PMMA, block copolymer, solvent annealing, free energy model

Disciplines

Engineering | Physical Sciences and Mathematics

Creative Commons License

This work is licensed under a Creative Commons Attribution-Share Alike 4.0 License.

This technical report is available at ScholarlyCommons: https://repository.upenn.edu/scn_protocols/54

Dynamics of Directed Self-Assembly of PS-b-PMMA during Solvent Annealing

Hiromichi Yamamoto[1, a)]
[1]*Singh Center for Nanotechnology, University of Pennsylvania*
3205 Walnut St. Philadelphia, PA 19104

(Dated: Received 18 January 2019; accepted 6 February 2019)

The graphoepitaxy of symmetric PS-*b*-PMMA BCP film on the PS 60 mol% brush layer is carried out using the chemically homogeneous topological pattern of SiO_2 layer and the home-made solvent annealing tool. It is confirmed by atomic force microscopy that PS-*b*-PMMA film on the periphery of the trench flows into the trench during the solvent annealing, so that the film thickness in the trench is thicker than that on the un-patterned area. The solvent annealing time dependence indicates the lamellar orientation in the trench changes from a mixture of the lamellar domain parallel and perpendicular to the side walls to the lamellar domain parallel to the side walls, and then changes back to the mixture, although the lamellar orientation perpendicular to the substrate remains the same. This result is also discussed with a free energy model for confined di-block copolymer. The lamellar domain perpendicular to the substrate is rationalized by confinement between the "neutral" film/air interface and the neutral PS 60 mol% brush layer. The lamellar domain parallel to the side walls indicates that the surface tensions of PS and PMMA blocks absorbing solvent vapor with the PS 60 mol% brush layer are not the same during the solvent annealing at 55 °C. Furthermore, the free energy difference between the parallel and perpendicular orientations is supposed to fluctuate due to the dynamics of PS-*b*-PMMA molecules by the solvent annealing, so that the lamellar orientation results in either of the lamellar domain parallel, perpendicular, or the mixture.

Key Words: directed self-assembly, PS-*b*-PMMA, solvent annealing, free energy model

I. Introduction

Directed self-assembly (DSA) of block copolymer (BCP) has been attracting great attention from industry and academia due to its low-cost, time-savings, and versatility when used in conjunction with a guide pattern created by conventional lithography techniques,[1–3] and has been considered as one of the most promising nanoscale lithography techniques. Up to now, sub-10 nm patterns of high-χ BCP (χ: Flory-Huggins interaction parameter) have been reported.[4,5] Furthermore, it is also possible to prepare ~20 nm diameter nanopores in the BCP film without guide pattern.[6] The goal of this project is to make this new technique available at Quattrone Nanofabrication Facility (QNF).

DSA of BCP forms lamellar or cylinder domains along the guide pattern on the substrate.[1–3] DSA on a chemically patterned guide is referred to as chemoepitaxy,[7–9] whereas DSA on a topographically patterned one is named by graphoepitaxy.[10–13] Figure 1 shows a schematic diagram of chemoepitaxy and graphoepitaxy when using BCP poly(styrene-block-methyl methacrylate) (PS-*b*-PMMA), which has been most extensively investigated for DSA. The form and the direction of PS and PMMA domains in chemoepitaxy are controlled by the interfacial interactions among PS, PMMA, the substrate, and the air, and by the BCP film thickness. On the other hand, in graphoepitaxy, the interaction with side walls is added to the above interactions.[11,12] The interfacial interaction (surface tension or surface energy) with the substrate can be modified by preparing an additional (underlying) layer, e.g. hydroxylated homopolymer or random copolymer,[14] self-assembled monolayers (SAMs) of modified alkyl chlorosilane[15] and ethylene glycol,[16] on the substrate. The additional layer is also referred to as the brush layer.

It is important to prepare the lamellar and cylinder domain perpendicular to the substrate suface for pattern transfer into the substrate using reactive ion etching or lift-off after removing PMMA domain from the BCP film. It has been reported that the lamellar and cylinder domain formations perpendicular to the substrate depend on the PS fractions of the brush layer and the BCP.[17,18] The lamellar domain perpendicular to the substrate is formed on the brush layer with PS 45 to 57 mol% for symmetric PS(52k)-*b*-PMMA(52k), where the number in the bracket represents average molecular weight. On the other hand, the PS cylinder domain perpendicular to the substrate can be prepared on the PS 55 to 57 mol% brush layer for asymmetric PS(20.2k)-*b*-PMMA(50.5k), while the PMMA cylinder domain is formed on the PS 59 to 72 mol% brush layer for asymmetric PS(50.5k)-*b*-

a) Electronic mail: hyam@seas.upenn.edu

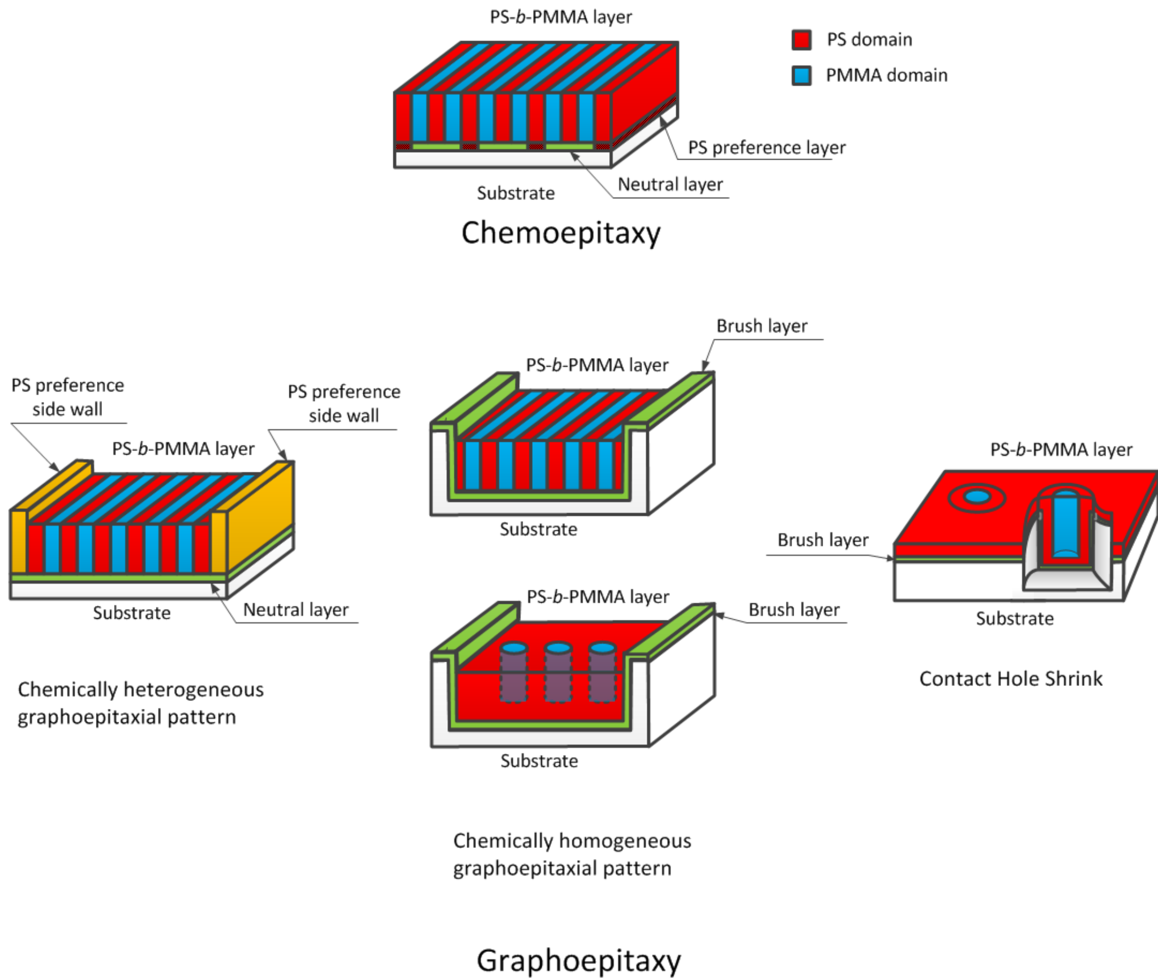

FIG. 1. A schematic diagram of chemoepitaxy and graphoepitaxy

PMMA(20.9k). Furthermore, ∼20 nm diameter cylinder domain can also be registered in nanopore guide pattern using Contact Hole Shrink technique,[19] as shown in Figure 1.

In chemoepitaxy, the PS and PMMA lamellar domains are induced one after the other by a PS preferentially striped pattern on the substrate to be aligned along the pattern, but perpendicular to the substrate.[6–8] In graphoepitaxy, chemically heterogeneous and homogeneous topographical patterns have been reported.[10,12] In the case of chemically heterogeneous graphoepitaxial pattern, PS preferred (Au) side walls are prepared on the non-preference (neutral) layer by conventional lithography, so that PS lamellar domain is aligned along PS preference side wall, but perpendicular to the substrate due to the neutral layer, and PMMA lamellar domain is also induced to be aligned along the PS lamellar domain. In the case of chemically homogeneous graphoepitaxial pattern, the brush layer is homogeneously prepared on the trench pattern. The lamellar domain in the trench can be controlled to be perpendicular to the substrate by adjusting the film thickness and the PS fractions of PS-*b*-PMMA and the brush layer.

This report describes graphoepitaxy of symmetric PS-*b*-PMMA films on the neutral brush layer in the various width trenches, using solvent annealing. Dependences of DSA of the BCP films on the solvent annealing time and on the trench width are also discussed with a free energy model for confined di-block copolymer.[20–23] Especially, the solvent annealing time dependence shows the orientation transition of the lamellar domains from perpendicular to parallel to the side wall, suggesting that the lamellar domain perpendicular to the side wall is still metastable due to dynamics of the PS-*b*-PMMA molecules by solvent annealing.

II. Experimental Section

A. Materials

Symmetric PS-b-PMMA (poly-methyl methacrylate rich in syndiotactic contents $>$ 78 or 80 %) with the average molecular weight Mn of poly-styrene = 33,000, Mn

of poly-methyl methacrylate = 33,000, and polydispersity index (PDI) =1.09 (polymer domain spacing L_0 = 36 nm) was purchased from Polymer Source, and was used as received. Hydroxyl-terminated random copolymer poly(styrene-r-methyl methacrylate), α-hydroxyl-ω-tempo moiety terminated, was also purchased from Polymer Source, and was used as received. The PS content was 60 mol% (Mn = 5,400 and PDI = 1.40). A CMOS grade toluene (trace impurity level, 10-200 ppb) was purchased from J. T. Baker, and was used as-received as solvent.

B. Deposition of 100 nm thick silicon oxide film

A (100) Si wafer was sonicated in acetone and isopropyl alcohol (IPA) for 5 min each, and then dried using a nitrogen gun. A 100 nm thick amorphous silicon oxide was deposited onto the Si wafer, using Oxford Plasma Lab 100 (Plasma Enhanced Chemical Vapor Deposition (PECVD)).

C. Trench guide pattern

100 nm thick PMMA film was spin coated on the 100 nm thick SiO_2 layer on the Si substrate, followed by baking it at 180 °C for 5 min on a hot plate. E-beam writing of 30 to 400 nm wide and 10 μm long trenches was carried out using Elionix ELS-7500EX with the following condition: an acceleration voltage of 50 kV; a beam current of 100 pA; an objective lens aperture of 40 μm; the e-beam dose = 200 $\mu C/cm^2$ in the area of 300 x 300 m^2 with the total dots of 60000 x 60000. The proximity effect correction was done using BEAMER (GenISys), and thus, e-beam exposure was not constant. The exposed PMMA film was developed in a 3:1 (v/v) mixture of IPA and de-ionized (DI) water for 60 sec. The sample developed was rinsed with IPA. The SiO_2 film was dry-etched $\sim$50 nm deep through the developed PMMA film at 65 mTorr with 20 sccm of CF_4 gas flow at 150 W RF power, using Oxford 80 plus RIE. The etching depth of $\sim$50 nm was determined using DI Dimension 3000 Atomic Force Microscopy (AFM) or Zygo NewView 7300 Optical Profilometer. After the etching, the PMMA film was stripped with sonication in acetone, and its residue was removed by piranha solution,[24] as described below.

D. Grafting the brush-OH film on the hydroxylated silicon oxide surface on Si wafer

The 100 nm thick silicon oxide films were hydroxylated by treatment of nitric acid (70 wt%) or piranha solution at 70-80 °C for 30-40 min.[25] O_2 plasma treatment was not carried out for the hydroxylation, due to possible cross-contamination in the tool frequently used in QNF. The samples hydroxylated were sonicated in DI water for 2 min, and then dried using nitrogen gun. A $\sim$20 nm thick brush-OH film was spin coated on the 100 nm thick SiO_2 layer on the Si substrate from the a 0.9 wt% toluene solution, and annealed at 190 °C in the oven filled with N_2 or in vacuum overnight or longer. After annealing, the unreacted brush-OH polymer was removed by repeated 30 min sonication in toluene (3 times). The thickness of the brush layer was 3 to 5 nm.

E. Film preparation of BCPs using solvent annealing

15, 22, and 42 nm thick PS-b-PMMA films were spin coated at 3000, 3500, and 3200 rpm on the brush layers grafted on the SiO_2 layers from 0.45, 0.78, and 1.52 wt% PS-b-PMMA toluene solutions, respectively. The PS-b-PMMA films were annealed at 55 °C for various time periods, using a home-made conventional solvent annealing tool. The solvent annealing is an annealing method to process self-assembly of BCP for a short time,[26–30] while it takes a long time for the thermal annealing using an oven to process the BCP film.[31] Self-assembly of BCP can occur in a closed system where the solvent vapor is filled, due to increase in the mobility of the polymer absorbing the solvent. Figure 2 shows photographs of the solvent annealing tool used in this study. Toluene was filled just below the sample chuck in the chamber. Vapor pressure of toluene in the chamber was determined by the temperature of the surrounding oil bath.

FIG. 2. Photographs of a conventional solvent annealing tool in this study; (a) overview; (b) the inside of the solvent annealing tool. The solvent temperature is controlled by an oil bath.

F. Measurements

The BCP films for the thickness measurements were separately spin coated on blank Si wafers. Film thicknesses of silicon oxide, BCP, and brush layer were determined, respectively, using Woollam VASE ellipsometer. Simulation model was Cauchy model. Scanning electron microscope (SEM) images were measured using JOEL JSM-7500F, and atomic force microscopy (AFM) images were also measure in a tapping mode using DI Dimension 3000. The PMMA portion of the BCP films was removed for SEM measurements by oxygen plasma at $\sim$170 mTorr with 10 sccm of oxygen gas flow at 40 W RF power (base pressure = $\sim$50 mTorr), for 3 min, using Anatech SCE-108 Barrel Asher.

III. A free energy model for confined di-block copolymer

Turner[20] and Walton et al.[21] described the equilibrium behavior of the melting state of symmetric A-B di-block copolymer confined between two hard walls in the ordered regime, the strong segregation limit, using a free

energy model including elastic energy of polymer and energies related to the surface tensions (or surface energies) among A block, B block, and two hard walls. They discussed lamellar orientation parallel and perpendicular to the walls with difference in surface tensions and BCP film thickness. Control of lamellar orientation to the substrate has also experimentally been confirmed using top coat on the BCP polymer film.[22,23] Assuming that the BCP film is sandwiched between the top and bottom walls, the free energies of the lamellar orientations relative to the bulk equilibrium free energy F_0 are given by the following equations:

$$\frac{F_{//\text{-SYM}}}{F_0} = \frac{1}{3}[(\frac{d}{n})^2 + \frac{2n}{d} + \frac{1}{d}(\frac{\gamma_{\text{A-Top}} + \gamma_{\text{A-Bottom}}}{\gamma_{\text{AB}}})] \quad (1)$$

$$\frac{F_{//\text{-ANTI}}}{F_0} = \frac{1}{3}[(\frac{d}{n+0.5})^2 + \frac{2(n+0.5)}{d} + \frac{1}{d}(\frac{\gamma_{\text{A-Top}} + \gamma_{\text{A-Bottom}}}{\gamma_{\text{AB}}})] \quad (2)$$

$$\frac{F_{\perp}}{F_0} = \frac{1}{3}[3 + \frac{1}{2d}(\frac{\gamma_{\text{A-Top}} + \gamma_{\text{B-Top}} + \gamma_{\text{A-Bottom}} + \gamma_{\text{A-Bottom}}}{\gamma_{\text{AB}}})] \quad (3)$$

where $F_{//\text{-SYM}}$ and $F_{//\text{-ANTI}}$ are the free energies for the lamellar orientation parallel to the walls when the top and bottom lamellae are the same (symmetric wetting) and different (anti-symmetric wetting), respectively, and $F_{\perp}$ is the free energy for the lamellar orientation perpendicular to the walls. $d = D/L_0$ is a normalized BCP film thickness by L_0, D is the BCP film thickness, n is an integer, and γ represents an energy related to the surface tension among A and B blocks and the walls. The perpendicular orientation is favored over the parallel one when $F_{\perp} < F_{//}$.[20–23] The subtraction of $F_{\perp}$ from $F_{//}$ gives the following equations:

$$\frac{F_{//\text{-SYM}} - F_{\perp}}{F_0} = \frac{1}{3}[(\frac{d}{n})^2 + \frac{2n}{d} - 3 + \frac{1}{2d}(\frac{\Delta\gamma_{\text{Top}} + \Delta\gamma_{\text{Bottom}}}{\gamma_{\text{AB}}})] \quad (4)$$

$$\frac{F_{//\text{-ANTI}} - F_{\perp}}{F_0} = \frac{1}{3}[(\frac{d}{n+0.5})^2 + \frac{2(n+0.5)}{d} - 3 + \frac{1}{2d}(\frac{\Delta\gamma_{\text{Top}} - \Delta\gamma_{\text{Bottom}}}{\gamma_{\text{AB}}}\gamma_{\text{AB}})] \quad (5)$$

where

$$\Delta\gamma_{\text{Top}} \equiv \gamma_{\text{A-Top}} - \gamma_{\text{B-Top}} \quad (6)$$

$$\Delta\gamma_{\text{Bottom}} \equiv \gamma_{\text{A-Bottom}} - \gamma_{\text{B-Bottom}} \quad (7)$$

If the top and bottom walls are the same, and neutral with the A and B blocks ($\gamma_{\text{A}} = \gamma_{\text{B}}$), then $F_{//}$ - $F_{\perp} >$ 0, namely the perpendicular orientation to the walls, is always favored. If the surface tension of A block with the wall is smaller than that of B block ($\gamma_{\text{A}} < \gamma_{\text{B}}$), then the region of the parallel orientation to the wall emerges around the commensurate thickness.[20–23] This will also be discussed later with the experimental result.

IV. Results and Discussion

A. Self-assembly of PS-b-PMMA films around the trench

The morphology of BCP film depends on the interface interaction and the film thickness, as described above. Polymer chain compression and stretching are controlled by incommensurability between the film thickness and the polymer domain spacing, and are released by the formation of islands and holes or by the formation of cylinders or lamellae, depending on the entropic frustration of polymer. When the film thickness is commensurate with L_0, the wetted BCP film is obtained. Otherwise, the dewetted BCP film is normally observed. In other words, self-assembly of BCP is very sensitive to the film thickness. Figure 3 shows SEM images of 15, 22, and 42 nm thick PS-*b*-PMMA films on the PS 60 mol% brush layer on the patterned SiO_2 layer; (a) 42 nm thick, zoom out; (b) 42 nm thick, zoom in; (c) 22 nm thick, zoom in; (d) 15 nm thick, zoom in. As can be seen in Figure 3(a) to 3(c) for the 22 and 42 nm thick PS-*b*-PMMA films, the fingerprint structure is observed on the un-patterned area (unconfined area), as a result of self-assembly, whereas the featureless structure is shown in the trenches (confined area). On the other hand, Figure 3(d) for the 15 nm thick PS-*b*-PMMA film shows the featureless structure on the unconfined area around the confined area, but clearly exhibits the fingerprint structure in the confined area.

Furthermore, the grain structure of the SiO_2 layer is also revealed on the periphery of the confined area, as shown in Figure 3(d), indicating that the PS-*b*-PMMA film goes away from the periphery of the confined area during the solvent annealing. On the other hand, the featureless structure in the confined area in Figures 3(a) to 3(c) does not show any grain structure of the SiO_2 layer, manifesting that PS-*b*-PMMA film is filled in the confined area. It has been confirmed that the fingerprint and featureless structures on the PS 60% brush layer are the lamellar domains perpendicular and parallel to the substrate, respectively.[10,12] Thus, the featureless structure in the confined area in Figures 3(a) to 3(c) should be the lamellar domain parallel to the substrate. Figure 4 shows AFM images of the cross-sections of the ∼50 nm depth 100 nm width trench patterns of the SiO_2 layer with and without 22 nm thick PS-*b*-PMMA films on the substrate; (a) trenches without PS-*b*-PMMA film; (b) trenches filled with PS-*b*-PMMA film. Figure 4(c) shows a schematic diagram of the cross section of the trench depicted by the AFM information. The film thickness in the confined area is not uniform to be 46 to 68 nm, whereas the film thickness on the unconfined area is uniform to be 22 nm, as shown in Figure 4(c). Considering

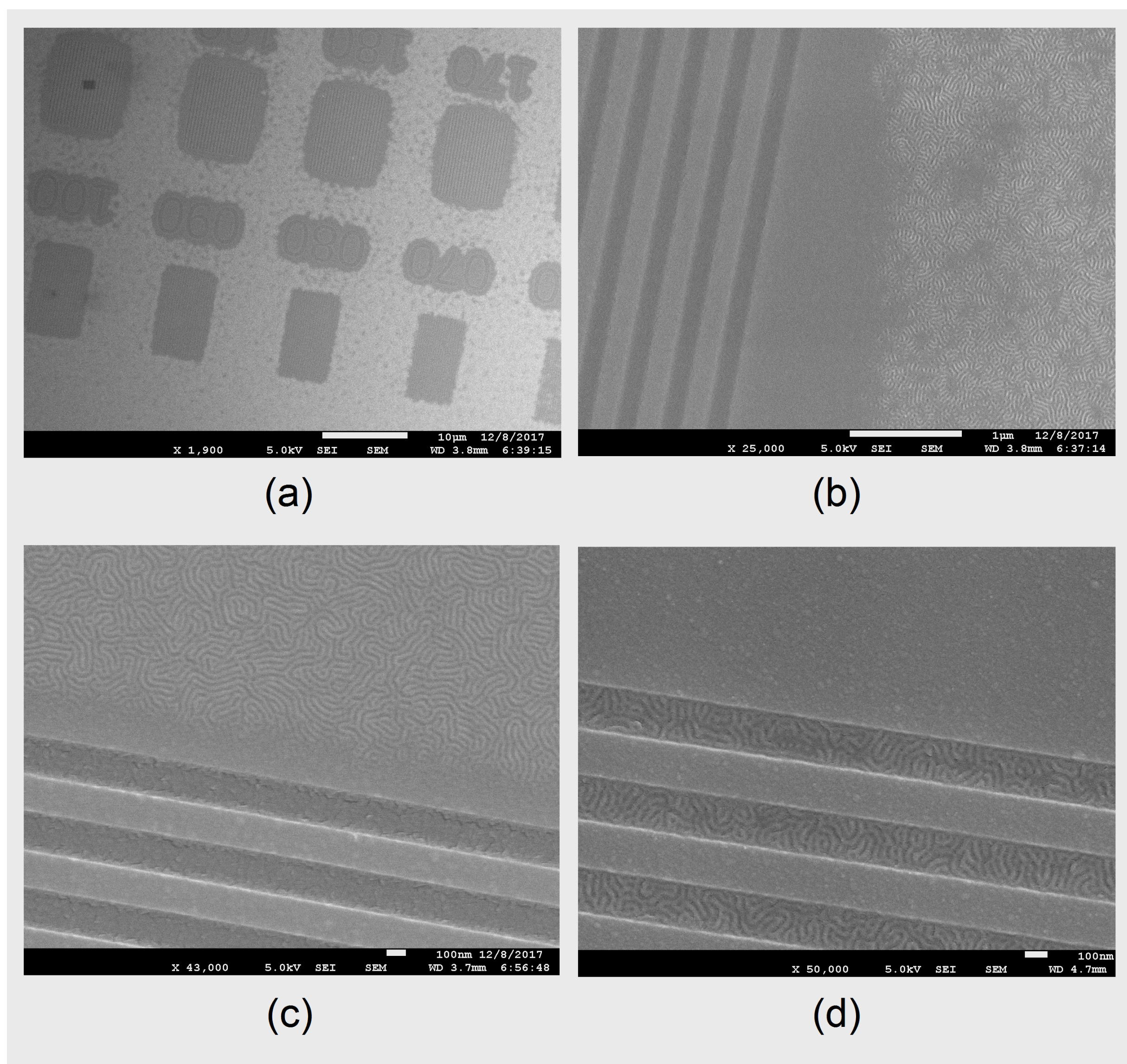

FIG. 3. SEM images of various thick PS-*b*-PMMA films on the brush layer on the patterned SiO_2 layer; (a) 42 nm thick, zoom out; (b) 42 nm thick, zoom in; (c) 22 nm thick, zoom in; (d) 15 nm thick, zoom in. The solvent annealing condition is 55 °C for 20 min.

the high mobility of the polymer molecules during the solvent annealing, the polymer molecules on the periphery of the trench would move down to the trench, so that the SiO_2 layer on the periphery of the confined area must be exposed, as shown in Figure 3(d), when the very thin PS-*b*-PMMA film is solvent annealed.

B. Solvent annealing time dependence

Hereafter, the lamellar domains parallel and perpendicular to the substrate are shown in the subscript to be lamellar$_{//}$ and lamellar$_{\perp}$, respectively, while the lamellar domains parallel and perpendicular to the side wall are represented in the superscript to be lamellar$^{//}$ and lamellar$^{\perp}$, respectively. Figure 5 shows SEM images of DSA of PS-*b*-PMMA films on the PS 60% brush layers in the 180 nm width ($= 5L_0$) trench of the SiO_2 layers when spin-coating 15 nm thick PS-*b*-PMMA film. The PS-*b*-PMMA films were solvent annealed at 55 °C for (a) 30 min, (b) 1, (c) 2, (d) 3, and (e) 4 hours. Figure 5(a) shows a mixture of the lamellar$_{//}$ (featureless) and lamellar$_{\perp}$ (fingerprint) in the confined area for 30 min annealing, as discussed above. The lamellar$_{\perp}$ also exhibits a mixture of the lamellar$_{\perp}{}^{//}$ and lamellar$_{\perp}{}^{\perp}$ in the confined area. Figure 5(b) indicates that the lamellar$_{//}$ disappears, and that the lamellar$_{\perp}$ shows a random orientation to the side walls for 1 hour annealing. Figure 5(c) and 5(d) show that the lamellar$_{\perp}{}^{//}$ becomes dominant over the lamellar$_{\perp}{}^{\perp}$ for 2 and 3 hour annealing. Especially figure 5(d) exhibits that most of the lamellar domains are the lamellar$_{\perp}{}^{//}$. Figure 6 indicates (a)

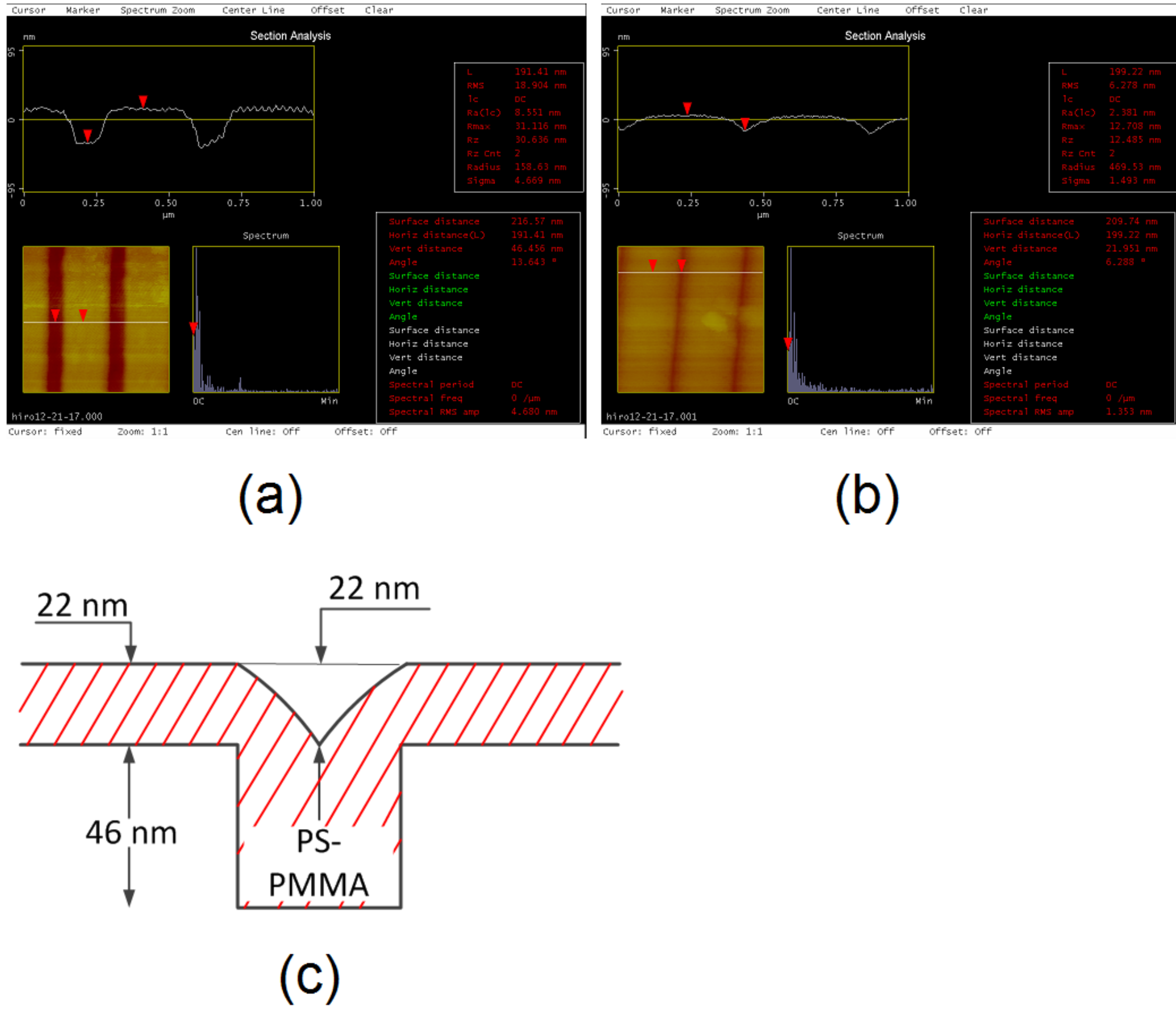

FIG. 4. AFM (tapping mode) images and their cross-sections of the 46 nm depth 100 nm width trench patterns of the SiO_2 layer with and without 22 nm thick PS-*b*-PMMA film in their trenches; (a) trenches without PS-*b*-PMMA film; (b) trenches filled with PS-*b*-PMMA film; (c) a schematic diagram of the cross section of the trench depicted by the AFM information. No brush layer was prepared on the substrates.

zoom-out and (b) zoom-in SEM images of PS-*b*-PMMA film for 3 hours annealing, revealing that the lamellar$_\perp{}^\perp$ domain disappears in the 4 μm x 5 μm area although a few small defects are still observed. On the other hand, figure 5(e) exhibits that a mixture of the lamellar$_\perp{}^{//}$ and lamellar$_\perp{}^\perp$ domains show up again for the 4 hour annealing.

Figure 7 shows $(F_{//} - F_\perp)/F_0$ vs the film thickness normalized by L_0 when $\Delta\gamma_{\mathrm{Top}}$ is changed, but $\Delta\gamma_{\mathrm{Bottom}} = 0$, exhibited by W. J. Durand *et al.*[23] The free energy of the lamellar orientation parallel to the wall $F_{//}$ for the symmetric wetting is always larger than that perpendicular to the wall $F_\perp$ (i.e. $F_{//} - F_\perp > 0$) when the top and bottom walls are neutral with the A and B blocks ($\gamma_{\mathrm{A}} = \gamma_{\mathrm{B}}$), namely the perpendicular orientation to the walls is always favored, although $F_{//} - F_\perp$ decreases with increase in the film thickness. If the surface tension of A block with the wall is not equal to that of B block ($\gamma_{\mathrm{A}} \neq \gamma_{\mathrm{B}}$), then the region of the parallel orientation to the wall shows up around the commensurate thickness.[20–23]

In the chemically homogeneous topological pattern as this study, the BCP film is considered to be confined between the film/air interface and the substrate with the brush layer on its surface in the z-direction, and between the side walls with the brush layers on their surfaces in the x-direction.[10,12] In addition, the surface tensions of PS and PMMA blocks with PS 60 mol% brush layer have been reported to be almost the same ($\gamma_{\mathrm{PS}} = \gamma_{\mathrm{PMMA}}$ at $f_{\mathrm{PS}} = 0.57$ at 170 °C, where f_{PS} is a PS fraction of the brush layer).[32] In fact, in the z-direction, the lamellar$_\perp$ on the PS 60% brush layer has been reported to be independent of the film thickness, which is rationalized by

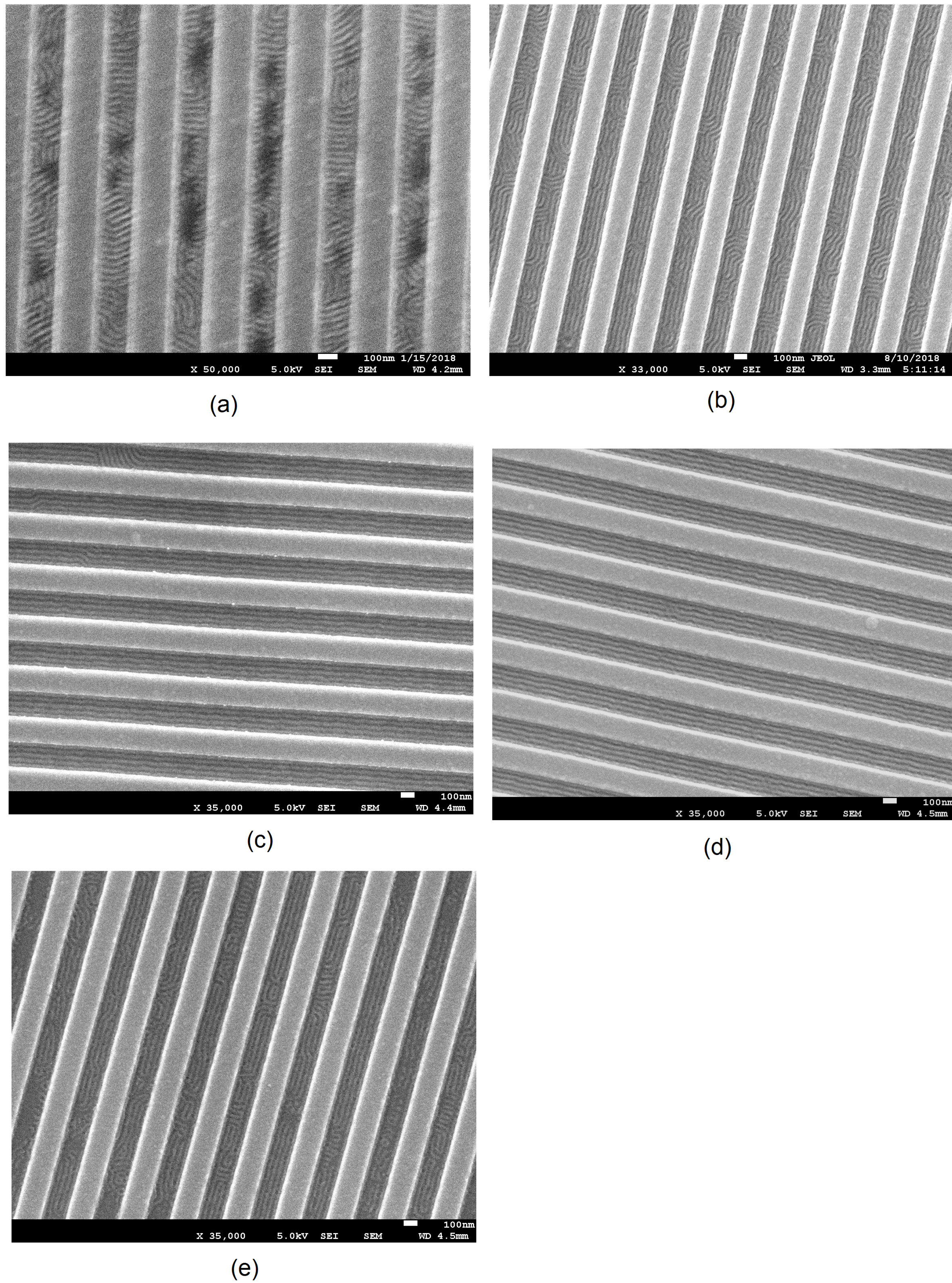

FIG. 5. SEM images of directed self-assembly of PS-*b*-PMMA films on the brush layers in the 180 nm width ($= 5L_0$) trench of the SiO_2 layers. The PS-*b*-PMMA films were solvent annealed at 55 °C for (a) 30 min, (b) 1, (c) 2, (d) 3, and (e) 4 hours.

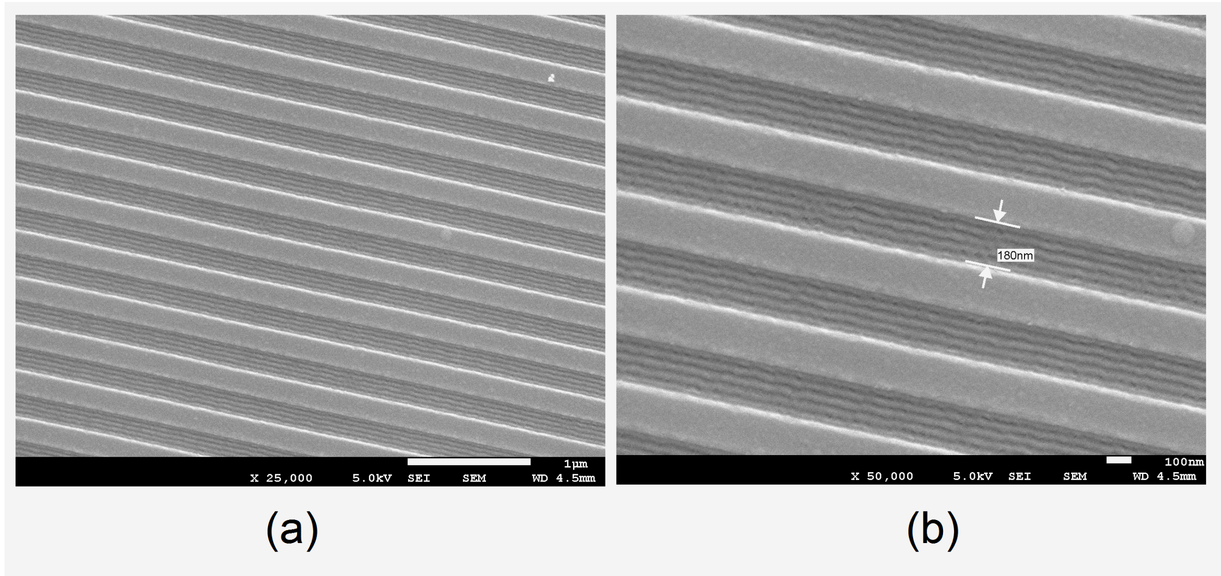

FIG. 6. SEM images of directed self-assembly of PS-b-PMMA film on the brush layers in the 180 nm width ($=5L_0$) trench of the SiO2 layers; (a) x25,000; (b) x50,000. The PS-b-PMMA film was solvent annealed at 55 °C for 3 hours. Some defects are still observed.

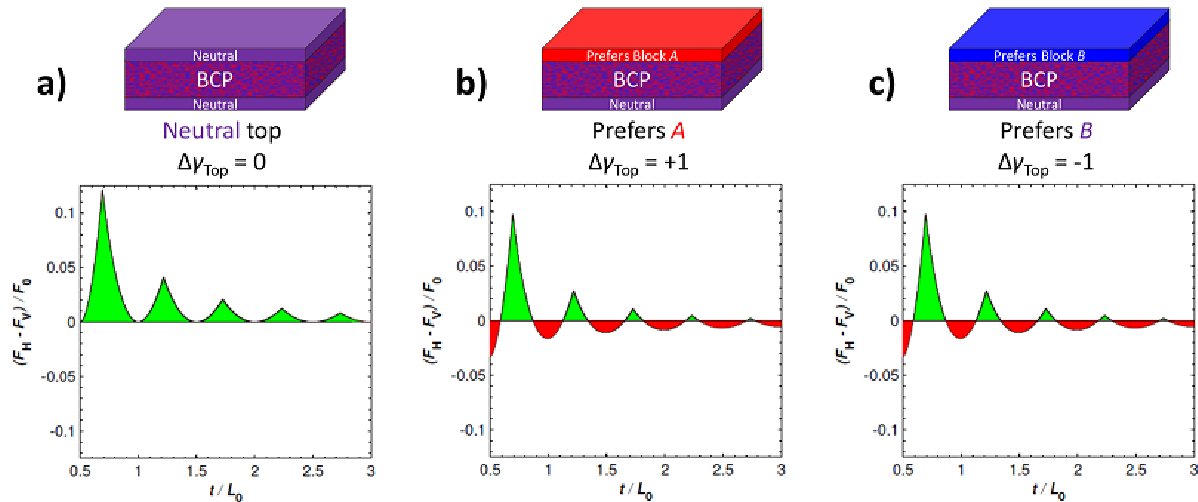

FIG. 7. $(F_{//} - F_{\perp})/F_0$ vs film thickness normalized by L_0 when $\Delta\gamma_{\text{Top}}$ is changed, but $\Delta\gamma_{\text{Bottom}} = 0$. The green area indicates the region of the lamellar perpendicular to the wall, whereas the red area depicts the region of the lamellar parallel to the wall. See the detail in Ref.23.

confinement between the "neutral" film/air interface and the neutral PS 60 mol% brush layer.[12]

In the x-direction of the trench, the BCP film is confined by the PS 60 mol% brush layers on the side walls, meaning that the lamellar$_{\perp}{}^{\perp}$ should always be observed, according to the above theory. However, Figure 5 clearly indicates that the lamellar orientation in the $5L_0$ width trench changes from the mixture of the lamellar$_{\perp}{}^{//}$ and lamellar$_{\perp}{}^{\perp}$ to the lamellar$_{\perp}{}^{//}$, and then changes back to the mixture of the lamellar$_{\perp}{}^{//}$ and lamellar$_{\perp}{}^{\perp}$, depending on the solvent annealing time. Especially the lamellar$_{\perp}{}^{//}$ indicates that the surface tensions of PS and PMMA blocks absorbing solvent vapor with the PS 60 mol% brush layer are not the same during the solvent annealing at 55 °C because the lamellar$_{\perp}{}^{//}$ should not appear if $\gamma_{\text{PS}} = \gamma_{\text{PMMA}}$. Furthermore, the free energy difference $F_{//}$ - $F_{\perp}$ at the $5L_0$ width, which should be very close to 0, as inferred in Figure 7, is supposed to fluctuate due to the dynamics of PS-b-PMMA molecules by the solvent annealing, so that the lamellar orientation results in either of the lamellar$_{\perp}{}^{//}$, the lamellar$_{\perp}{}^{\perp}$, or the mixture. Actually, it has also been reported that a

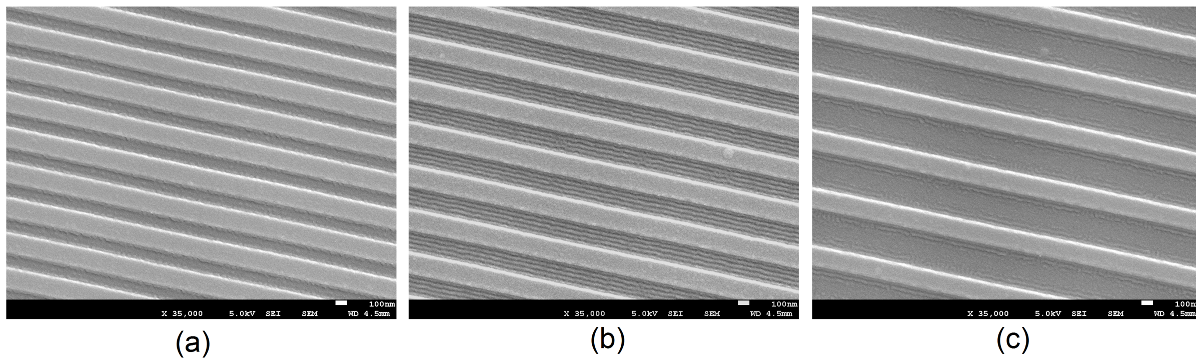

FIG. 8. SEM images of PS-b-PMMA films on the PS 60 mol% brush layer on the patterned SiO_2 layer; (a) 120 nm width (=3.3L_0), (b) 180 nm width (=5L_0); (c) 310 nm width (=8.6L_0). PS-b-PMMA film was solvent annealed at 55 °C for 3 hours. The film thickness on the un-patterned area is 15 nm.

mixture of the lamellar$_\perp{}^{//}$ and the lamellar$_\perp{}^{\perp}$ or only the lamellar$_\perp{}^{\perp}$ is formed on the PS 60 mol% brush layer in the trench by thermal annealing at 220 °C.[10,12]

C. Trench width dependence

The PS-b-PMMA film thickness in the trench should decrease with increase in the trench width, as shown above. Figure 8 shows SEM images of PS-b-PMMA films on the PS 60 mol% brush layer in (a) 120 nm width (=3.3L_0), (b) 180 nm width (=5L_0), (c) 310 nm width (=8.6L_0) trenches of the SiO_2 layer. The PS-b-PMMA films were solvent annealed at 55 °C for 3 hours. The BCP film thickness on the un-patterned area is 15 nm. Figures 8(a) and (c) show the lamellar$_{//}$, indicating that the surface tensions of PS and PMMA blocks with the film/air interface are not the same, as shown in Figure 7. In addition, the film thicknesses in the 120 and 310 nm width trenches should be close to the commensurate thickness. Furthermore, the lamellar$_\perp$ is also observed near the side walls, confirming flow induced effects.[12] On the other hand, Figure 8(b) indicates the lamellar$_\perp$, which should have the incommensurate thickness, according to figure 7.

V. Summary

The graphoepitaxy of symmetric PS-b-PMMA BCP film on the PS 60 mol% brush layer was carried out using the chemically homogeneous topological pattern of SiO_2 layer and the home-made solvent annealing tool. It was confirmed by AFM that PS-b-PMMA film on the periphery of the trench flows into the trench during the solvent annealing, so that the film thickness in the trench is thicker than that on the un-patterned area. The solvent annealing time dependence indicated the lamellar orientation in the $5L_0$ width trench changes from the mixture of the lamellar$_\perp{}^{//}$ and lamellar$_\perp{}^{\perp}$ to the lamellar$_\perp{}^{//}$, and then changes back to the mixture of the lamellar$_\perp{}^{//}$ and lamellar$_\perp{}^{\perp}$.The result was also compared with the free energy model for confined di-block copolymer. The lamellar$_\perp$ was rationalized by confinement between the neutral film/air interface and the neutral PS 60 mol% brush layer. In addition, the lamellar$_\perp{}^{//}$ indicated that the surface tensions of PS and PMMA blocks absorbing solvent vapor with the PS 60 mol% brush layer are not the same during the solvent annealing at 55 °C. Furthermore, the free energy difference $F_{//}$ - $F_\perp$ at the $5L_0$ width is supposed to fluctuate due to the dynamics of PS-b-PMMA molecules by the solvent annealing, so that the lamellar orientation results in either of the lamellar$_\perp{}^{//}$, the lamellar$_\perp{}^{\perp}$, or the mixture. The trench width dependence showed the lamellar$_{//}$ in the 120 and 310 nm width trenches and the lamellar$_\perp$ in the 180 nm width trench, indicating that the film thicknesses in the 120 and 310 nm width trenches are close to the commensurate thickness, whereas that in the 180 nm width trench is the incommensurate thickness.

VI. Acknowledgements

The author is grateful to Dr. S. Nicaise for useful suggestion on the home-made solvent annealing tool. This work was supported by the National Science Foundation (Grant NNCI-1542153).

[1] M. Gopinadhan H. Hu and C. O. Osuji. *Soft Matter*, 10:3867, 2014.
[2] M.A. Morris. *Microelectron. Eng.*, 132:207, 2015.
[3] S. Ji, L. Wan, C.-C. Liu, and P. F. Nealey. *Prog. Polym. Sci.*, 54-55:76, 2016.
[4] N. Kihara, Y. SEino, H. Sato, Y. Kasahara, K. Kobayashi, K. Miyagi, S. Minegishi, K. Yatsuda, T. Fujiwara, N. Hirayanagi, H. Kanai, Y. Kawamonzen, K. Kodera, T. Azuma, and T. Hayakawa. *J. Micro/Nanolith. MEMS MOEMS*, 14:023502, 2015.
[5] W. J. Durand, G. Blachut, M. J. Maher, S. Sirard, S. Tein, M. C. Carlson, Y. Asano, S. X. Zhou, A. P. Lane, C. M. Bates, C. J. Ellison, and C. G. Willson1. *J. Polym. Sci., Part A: Polym. Chem.*, 53:344, 2015.
[6] C. Zhou, T. S.-Peretz, M. E. Oruc, H. S. Suh, G. Wu, and P. F. Nealey. *Adv. Funct. Mater.*, 27:1701756, 2017.
[7] M. P. Stoykovich, H. Kang, K. C. Daoulas, G. Liu, C. C. Liu, J. J. de Pablo, M. Mueller, and P. F. Nealey. *ACS Nano*, 1:168, 2007.

[8] J. Y. Cheng, C. T. Rettner, D. P. Sanders, H. C. Kim, and W. D. Hinsberg. *Adv. Mater.*, 20:3155, 2008.

[9] R. Ruiz, H. M. Kang, F. A. Detcheverry, E. Dobisz, D. S. Kercher, T. R. Albrecht, J. J. de Pablo, and P. F. Nealey. *Science*, 321:936, 2008.

[10] S. M. Park, M. P. Stoykovich, R. Ruiz, Y. Zhang, C. T. Black, and P. E. Nealey. *Adv. Mater.*, 19:607, 2007.

[11] J. Chai and J. M. Buriak. *ACS Nano*, 2:489, 2008.

[12] E. Han, H. Kang, C.-C. Liu, P. F. Nealey, and P. Gopalan. *Adv. Mater.*, 22:4325, 2010.

[13] M. Kim, E. Han, D. P. Sweatb, and P. Gopalan. *Soft Matter*, 9:6135, 2013.

[14] K. Sparnacci, D. Antonioli, V. Gianotti, M. Laus, F. F. Lupi, T. J. Giammaria, G. Seguini, and M. Perego. *ACS Appl. Mater. Interfaces*, 7:10944, 2015.

[15] R. D. Peters, X. M. Yang, T. K. Kim, and P. F. Nealey. *Langmuir*, 16:9620, 2000.

[16] D. Borah, M. Ozmen, S. Rasappa, M. T. Shaw, J. D. Holmes, and M. A. Morris. *Langmuir*, 29:2809, 2013.

[17] E. Han, K. O. Stuen, Y.-H. La, P. F. Nealey, and P. Gopalan. *Macromolecules*, 41:9090, 2008.

[18] J. N. L. Albert and T. H. Epps. *Mater. Today*, 13:24.

[19] F. Delachat, A. Gharbi, P. P. Barros, M. Argoud, C. Lapeyre, S. Bos, J. Hazart, L. Pain, C. Monget, X. Chevalier, C. Nicolet, C. Navarro, I. Cayrefourcq, and R. Tiron. *Proc. of SPIE*, 10144:101440O–1, 2017.

[20] M. S. Turner. *Phys. Rev. Lett.*, 69:1788, 1992.

[21] D. G. Walton, G. J. Kellogg, A. M. Mayes, P. Lambooy, and T. P. Russell. *Macromolecules*, 27:6225, 1994.

[22] C. M. Bates, T. Seshimo, M. J. Maher, W. J. Durand, J. D. Cushen, L. M. Dean, G. Blachut, C. J. Ellison, and C. G. Willson. *Science*, 338:775, 2012.

[23] W. J. Durand, M. C. Carlson, M. J. Maher, G. Blachut, L. J. Santos, S. Tein, V. Ganesan, C. J. Ellison, and C. G. Willson. *Macromolecules*, 49:308, 2016.

[24] A 3:1 (v/v) mixture of sulfuric acid (H_2SO_4, 95-98 wt%) and hydrogen peroxide (H_2O_2, 30 wt%).

[25] S. Guhathakurta and A. Subramanian. *J. Electrochem. Soc.*, 154:P136, 2007.

[26] S. Ji, L. Wan, C.-C. Liu, and P. F. Nealey. *Prog. Polym. Sci.*, 54-55:76, 2016.

[27] W. I. Park, K. Kim, H.-I. Jang, J. W. Jeong, J. M. Kim, J. Choi, J. H. Park, , and Y. S. Jung. *Small*, 8:3762, 2012.

[28] K. W. Gotrik, A. F. Hannon, J. G. Son, B. Keller, A. A. Katz, and C. A. Ross. *ACS Nano*, 6:8052, 2012.

[29] A. Tavakkoli K. G., S. M. Nicaise1, K. R. Gadelrab, A. A.-Katz, C. A. Ross, and K. K. Berggren. *Nat. Commun.*, 7:10518, 2016.

[30] D. Borah, M. T. Shaw, J. D. Holmes, and M. A. Morris. *ACS Appl. Mater. Interfaces*, 5:2004, 2013.

[31] H. Yamamoto. `https://repository.upenn.edu/scn_protocols/27/`. If the SiO2 layer was not e-beam lithographed before the hydroxylation, the thickness of the brush layer was 3 to 7 nm, depending on the process condition.

[32] P. Mansky, Y. Liu, E. Huang, T. P. Russell, and C. Hawker. *Science*, 275:1458, 1997.